Current Research in Microbial Sciences 4 (2023) 100181

Contents lists available at ScienceDirect

Current Research in Microbial Sciences

journal homepage: www.sciencedirect.com/journal/current-research-in-microbial-sciences

Impaired immune response and barrier function in GSPD-1-deficient *C. elegans* infected with *Klebsiella pneumoniae*

Wan-Hua Yang [a], Po-Hsiang Chen [b], Hung-Hsin Chang [c], Hong Luen Kwok [c], Arnold Stern [d], Po-Chi Soo [e], Jiun-Han Chen [c], Hung-Chi Yang [c,*]

[a] *Department of Pathology and Laboratory Medicine, Taipei Veterans General Hospital, Hsinchu Branch, Hsinchu, Taiwan*
[b] *Research Center for Chinese Herbal Medicine, Graduate Institute of Health Industry Technology, College of Human Ecology, Chang Gung University of Science and Technology, Taoyuan, Taiwan*
[c] *Department of Medical Laboratory Science and Biotechnology, Yuanpei University of Medical Technology, Hsinchu 30041, Taiwan*
[d] *Grossman School of Medicine, New York University, New York, NY, USA*
[e] *Department of Laboratory Medicine and Biotechnology, College of Medicine, Tzu Chi University, Hualien, Taiwan*

ARTICLE INFO

Keywords:
Klebsiella pneumoniae
Bacterial colonization
Tight junction
GSPD-1 *C. elegans*

ABSTRACT

gspd-1-RNAi knockdown *Caenorhabditis elegans* was used as an immune-compromised model to investigate the role of G6PD in host-pathogen interactions. A shorted lifespan, increased bacterial burden and bacterial translocation were observed in *gspd-1*-knockdown *C. elegans* infected with *Klebsiella pneumoniae* (KP). RNAseq revealed that the innate immune pathway, including *clc-1* and *tsp-1*, was affected by *gspd-1* knockdown. qPCR confirmed that tight junction *(zoo-1, clc-1)* and immune-associated genes (*tsp-1*) were down-regulated in *gspd-1*-knockdown *C. elegans* and following infection with KP. The down-regulation of antimicrobial effector lysozymes, including *lys-1, lys-2, lys-7, lys-8, ilys-2* and *ilys-3*, was found in *gspd-1*-knockdown *C. elegans* infected with KP. Deletion of *clc-1, tsp-1, lys-7*, and *daf-2* in *gspd-1*-knockdown *C. elegans* infected with KP abolished the shorten lifespan seen in the Mock control. GSPD-1 deficiency in *C. elegans* resulted in bacterial accumulation and lethality, possibly due to a defective immune response. These findings indicate that GSPD-1 has a protective role in microbial defense in *C. elegans* by preventing bacterial colonization through bacterial clearance.

1. Introduction

Glucose-6-phosphate dehydrogenase (G6PD) is a housekeeping gene from bacteria to human. As the rate-limiting enzyme in the pentose phosphate pathway (PPP), G6PD produces ribose-5-phosphate and NADPH for nucleic acid synthesis and reductive biosynthesis, respectively. The biological function of G6PD is essential for cell proliferation and organismal development (Yang et al., 2019). Insufficient G6PD due to mutations causes red cell-related clinical symptoms, including neonatal jaundice, favism, and drug or infection-induced hemolysis (Luzzatto and Seneca, 2014). Severe G6PD deficiency disrupts lipid metabolism and the permeability barrier in nematode embryos leading to embryonic lethality (Yang et al., 2020; Chen et al., 2017).

Caenorhabditis elegans is a free-living soil nematode and widely used for biomedical research because of many advantages, such as ease of culture, a transparent body for microscopy and tractable genetics (Jorgensen and Mango, 2002). The G6PD homologue of *C. elegans*, GSPD-1, shares high sequence similarity with the human counterpart (Yang et al., 2013). *gspd*-1-knockdown *C. elegans* exhibit several embryonic impairments, including a hatching defect, abnormal eggshell structure, enhanced permeability, defective polarity and cytokinesis (Chen et al., 2017). Despite the fact that G6PD is associated with the immune response and microbial infections (Yen et al., 2020; Yang et al., 2021), the role of G6PD in the host-pathogen interaction is largely unknown. *Klebsiella pneumoniae* (KP), a Gram-negative, facultative anaerobic bacillus, causes different types of healthcare-associated disorders (Panjaitan et al., 2021). KP is commonly found and harmless in the human intestine. While healthy individuals are rarely infected with KP, immuno-compromised individuals are highly susceptible to the infections (Paczosa and Mecsas, 2016).

The current study involved the investigation of the role of GSPD-1 during infection with KP. Specifically, shorten lifespan, increased

Abbreviations: GSPD-1, Glucose Six (6) Phosphate Dehydrogenase; NADPH, Nicotinamide adenine dinucleotide phosphate.

* Corresponding author.
E-mail address: hcyang@mail.ypu.edu.tw (H.-C. Yang).

https://doi.org/10.1016/j.crmicr.2023.100181

Available online 27 January 2023

bacterial burden and translocation were observed in *gspd*-1-knockdown *C. elegans* infected with KP. Several innate immune response and tight-junction (TJ)-related genes modulated by *gspd-1* status have been identified by transcriptomic analysis and PCR validation. The epistatic genetic studies showed that *daf-2* acts up-stream and *lys-7/clc-1/tsp-1* act down-stream of *gspd*-1. Mechanistically, *gspd-1* deficiency down-regulated lysozyme gene *lys-7*, causing defective bacterial clearance. GSPD-1 deficiency also down-regulated the TJ-related genes *clc-1* and *zoo-1*, leading to compromised barrier integrity of the digestive tract. The current work not only identified the key innate immune gene regulatory network modulated by GSPD-1 during KP infection, but also provided an immuno-compromised model for studying the mechanism of host-pathogen interactions.

2. Materials and methods

2.1. Bacteria and nematode culture

Bacterial strains, *Klebsiella pneumoniae* type strain (ATCC 13883) and *Escherichia coli* (HT115, OP50), were cultured on a rotatory shaker at 200 rpm and 37 °C in LB medium supplemented with appropriate antibiotics at the following final concentration: ampicillin (200 μg/mL). *C. elegans* strains N2 (wild type), CB1370 [*daf-2(e1370)*], CF1038 [*daf-16(mu86)*], VC3875 [*clc-1(gk3754)*], *RB2582* [*tsp-1(ok3594)*], and CB6738 [*lys-7(ok1384)*] were acquired from Caenorhabditis Genetics Center (University of Minnesota, Minneapolis, MN, USA). All *C. elegans* strains were maintained on Nematode growth medium (NGM) agar plates seeded with bacterial lawn (Incubator DBL120, DENG YNG) according to standard protocols (Stiernagle, 2006).

2.2. gspd-1 RNAi knockdown

RNAi knockdown was carried out by feeding dsRNA-expressed bacteria based on a recent report (Yang et al., 2020). Briefly, gravid hermaphrodites fed on *E. coli* OP50 were treated with 1% hypochlorite bleach and a 0.5 M sodium hydroxide solution. Eggs were washed and incubated in M9 buffer for 16 h to obtain synchronized L1 larvae, followed by culturing on NGM agar consisting of 1 mM IPTG, ampicillin (Sigma-Aldrich, St. Louis, MO, USA), and seeded with *E. coli* HT115 expressing a L4440 vector control (Mock) or a *gspd-1* RNAi (Gi) (Yang et al., 2013).

2.3. Cell culture

The human intestinal epithelial cell line, HCT116, was grown in RPMI supplemented with 10% FCS, antibiotics (100 units/ml penicillin and 100 mg/ml streptomycin) and 5% CO_2 at 37 °C. The generation of the G6PD-deficient cells was performed by using the G6PD inhibitors, 6-AN and DHEA (Thermo). The control cells were treated with DMSO.

2.4. Hiseq sequencing and data analysis

Total RNA was extracted from the Mock control and Gi *C. elegans* without KP infection at the 5th day of the adult stage by using TRIzol (Thermo). The quality of RNA was examined by nanodrop, Agilent Bioanalyzer 2100 and 1.5% agarose gel electrophoresis to guarantee purity and integrity of the RNA samples. The mRNA was enriched and used for the construction of a double-stranded library. RNA sequencing was performed by Illumina HiSeq. Raw reads were trimmed to remove low quality bases. Spliced transcript alignment was performed followed by transcripts reconstruction and estimation of transcripts abundance by Cuffquant. To determine the expression level of the genes, read sequences were compared with the *C. elegans* reference genome (Ensembl WBcel235). Normalized gene expression was performed by calculating the number of RNA-Seq Fragments Per Kilobase of transcript per total Million fragments mapped. Cuffdiff and CummeRbund were employed to identify the differentially expressed genes (DEGs) and to plot expression, respectively. The significantly expressed genes were selected based on the $\log_2$ fold change ≥ 1 and a P value < 0.05.

2.5. Lifespan assay

A *C. elegans* lifespan assay was performed at 20 °C based on standard protocols. In brief, ~40 L4 stage Mock or Gi *C. elegans* were fed with *E. coli* HT115 and were transferred to KP-seeded NGM agar plates supplemented with 50 μM 5-fluoro-2′-deoxyuridine (FUDR) (Thermo Scientific). This was considered as day 0. Live adult worms were transferred to fresh plates daily and their death was scored until no worms survived. The experiment was performed in triplicate and survival data was calculated by the Kaplan–Meir survival analysis in Prism (version 8.4) (GraphPad).

2.6. Reverse transcription and quantitative PCR (qPCR)

Total RNA of *C. elegans* or HCT116 cells was extracted using TRIzol (Thermo). cDNA was synthesized by the use of SuperScript III Reverse Transcriptase (Thermo) with 0.5 μg of oligo (dT)18 primer (Bioman Scientific, Taipei, Taiwan). Quantitative PCR was performed by using a StepOne (ABI) and a SYBR green reagent (KAPA, SIGMA). The thermal cycle program was as follows: 95 °C for 20 s, 40 cycles of 95 °C for 3 s, 60 °C for 30 s and 95 °C for 30 s. Primers were listed in the supplementary section (Table S1 and S2). The gene expression level was normalized to threshold cycle (Ct) values of the housekeeping gene (*ama-1*, for *C. elegans; β-actin* for HCT116 cells). The relative index ($2^{-\Delta\Delta Ct}$) was calculated by comparing the average expression levels for controls with the index defined as 1.0.

2.7. G6PD activity assay

The GSPD-1 activity of adult *C. elegans* was assayed spectrophotometrically at 340 nm by the reduction of $NADP^+$ as previously described (Yang et al., 2013). In brief, staged day 1 adults were harvested from an NGM agar plate by washing with PBS to remove bacteria. The worms were resuspended in extraction buffer (20 mM Tris–HCl, pH 8.0, 3 mM magnesium chloride, 1 mM EDTA, 0.02% β-mercaptoethanol, 1 mM ε-aminocaproic acid and 0.1% Triton X-100). The worm suspension was chilled immediately on ice and homogenized by a pellet pestle motor (Kontes). The crude lysates were centrifuged at 12,000 r.p.m. for 15 min at 4 °C (Z 233 MK-2, Hermle) and the supernatants (protein-containing lysate) were obtained. The Protein concentration of the lysate was determined by the Bradford method (Bio-Rad, Hercules, CA, USA). A typical assay mixture consisted of 100 mg of protein lysate in 0.2 ml of assay buffer (50 mM Tris–HCl pH 8, 50 mM $MgCl_2$, 4 mM $NADP^+$, 4 mM glucose 6-phosphate). The change of absorbance at 340 nm in each sample was measured spectrophotometrically for 15 min at 37 °C (SPECTROstar Nano, BMG Labtech).

2.8. Microscopy

The bacterial accumulation in *C. elegans* was visualized based on the detection of a red fluorescent protein (pBSK::Km::dsRED) labelled KP. In brief, staged adult hermaphrodites grown at 20 °C were harvested from NGM agar plates seeded with red fluorescent KP. These worms were washed with PBS and anesthetized with 2% levamisole followed by mounting on 2% agarose pads on glass slides. Fluorescent images were taken by using an epifluorescence microscope (Nikon Eclipse E400) coupled with an LED lamp (BioPioneer) and CMOS digital camera (FL-20, BioPioneer) and analyzed by imaging software (Image-Pro-Plus, Media Cybernetics).

2.9. Bacterial load assay

The bacterial load assay, modified from a protocol (Ayala et al., 2017), was measured based on the colony forming unit (CFU) of bacteria colonized in the *C. elegans* gut. In brief, staged L4 larvae of the Mock control or Gi *C. elegans* were transferred to a red fluorescent protein (pBSK::Km::dsRED) labelled KP-seeded NGM agar plates supplemented with 50 μg/ml kanamycin. After 2 days of infection, 50 live adult worms of each group were transferred to an Eppendorf tube containing 50 μl of PBS by using a worm picker made of an eyebrow hair. The samples were washed thrice with PBS to remove outside bacteria. The samples were homogenized by a pellet pestle motor (Kontes) trice. Each round consisted of 30 s homogenizations followed by a quick spin down with a desktop mini-centrifuge (Thermo). The worm lysates were centrifuged at 12,000 rpm for 15 min. Serial dilution (2X) of the worm lysates were prepared with sterilized PBS. 50 μl of each dilution was spread on an LB agar plate supplemented with 50 μg/ml kanamycin. After overnight incubation at 37 °C, bacterial colonies between 30 and 300 on a plate were counted and recorded. The number of CFU/worm was calculated as follows: CFU/worm in a given plate = (number of colonies X dilution factor)/50.

2.10. Statistical analysis

All statistical analyses were conducted using the Prism 8.4. version (GraphPad, San Diego, CA, USA). Data of three independent experiments were presented as the mean ± SD. The statistical difference between the control and the experimental groups was analyzed by the independent student's *t*-test. *P*-values below 0.05 were considered statistically significant.

3. Results

3.1. Effect of gspd-1 knockdown in C. elegans with KP infection

The lifespan of *gspd-1*-knockdown *C. elegans* infected with KP was significantly reduced compared with the Mock control infected with KP ($P = 0.0006$) (Fig. 1a). The shorten lifespan caused by *gspd-1*-

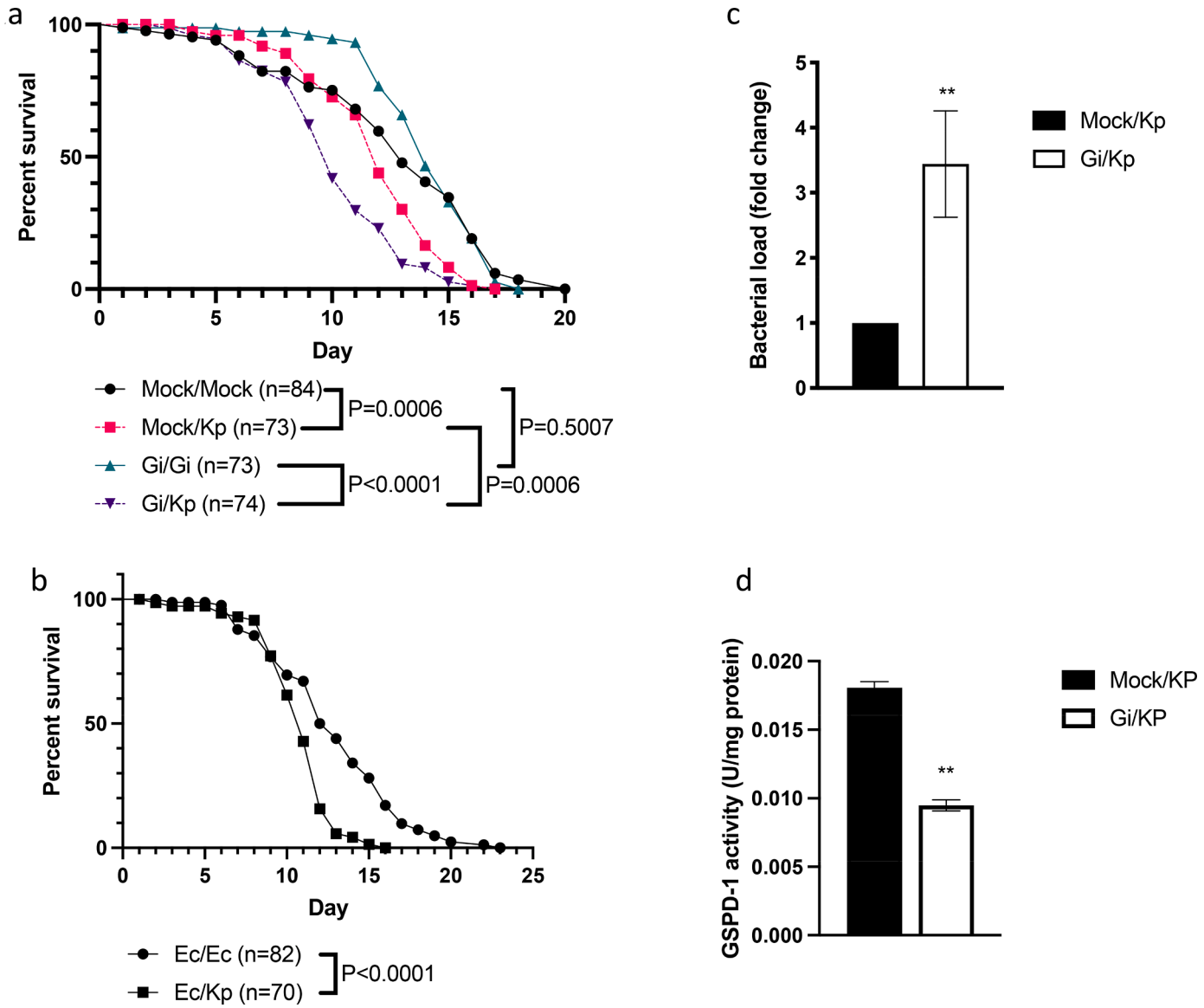

Fig. 1. Effects of bacterial diet on *C. elegans*. (a) Lifespan of the Mock control and *gspd-1* (RNAi) *C. elegans* infected with KP, (b) Lifespan of *C. elegans* with *E. coli* OP50 (Ec) and KP, (c) Bacterial burden of the Mock control and *gspd-1* (RNAi) *C. elegans* infected with KP. (d) GSPD-1 activity of the Mock control and *gspd-1* (RNAi) *C. elegans* infected with KP for 2 days.

knockdown was not observed with *E. coli* ($P = 0.5007$). Compared with *E. coli* OP50, KP significantly reduced the *C. elegans* lifespan ($P<0.0001$) (Fig. 1b). No difference in bacterial lawn avoidance between *E. coli* and KP was found in *C. elegans* (Figure S1). The bacterial load assay revealed that increased KP colonization was detected in *gspd-1*-knockdown *C. elegans* compared to the Mock control (Fig. 1c). The G6PD activity assay showed that reduced GSPD-1 activity was detected in *gspd-1*-knockdown *C. elegans* infected with KP compared to the Mock control (Fig. 1d). No difference of pharyngeal pumping between the Mock control and *gspd-1*-knockdown *C. elegans* infected with KP was found (Fig. S2).

The *gspd-1*-knockdown *C. elegans* infected with KP labeled with a red fluorescent protein was visualized by microscopy to examine how GSPD-1 deficiency affects bacterial colonization (Fig. 2). The difference in KP accumulation between the Mock control and *gspd-1*-knockdown *C. elegans* was not obvious upon short-term infection (less than 6 days-post-infection (dpi)). However, the distended foregut and increased KP accumulation were observed in both the Mock control and *gspd-1*-knockdown *C. elegans* upon long-term infection (8 - 13 dpi). Notably, from 10 dpi, KP was detected outside the foregut in both mock and *gspd-1*-knockdown *C. elegans*, indicating that KP disrupts barrier function of the alimentary tract (Fig. 2).

3.2. Genome-wide screening and validation of differentially expressed genes modulated by gspd-1 knockdown

The transcriptome of mock and *gspd-1*-knockdown *C. elegans* was analyzed by RNAseq to investigate the gene regulation network in GSPD-1 deficiency (Fig. 3). High-throughput sequencing revealed that using the selection criteria, 493 DEGs were modulated by GSPD-1 deficiency. Specifically, 202 up-regulated DEGs and 291 down-regulated DEGs were obtained. An enrichment analysis of gene ontology (GO) based on the DEGs showed that among the top 10 biological processes, the most significant one was the innate immune

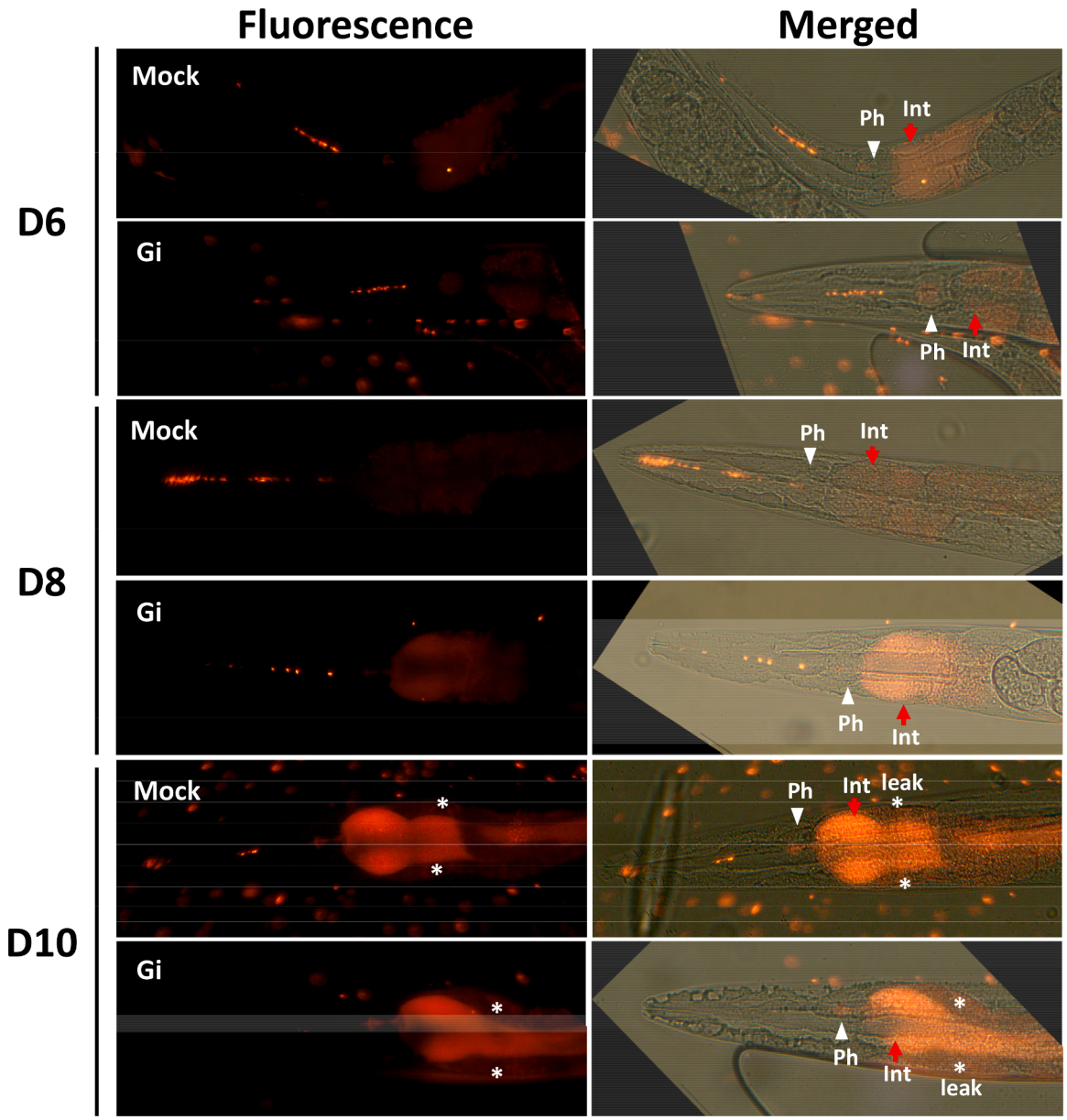

Fig. 2. Fluorescent microscopy of the Mock control and *gspd-1* (RNAi) *C. elegans* infected with KP. Infected worms were harvested at the indicated time. Red fluorescence represents the accumulation of KP. The white triangle mark indicates Pharynx (Ph) of *C. elegans*. The red arrowhead mark indicates intestine (Int) of *C. elegans*. * indicates KP leakage.

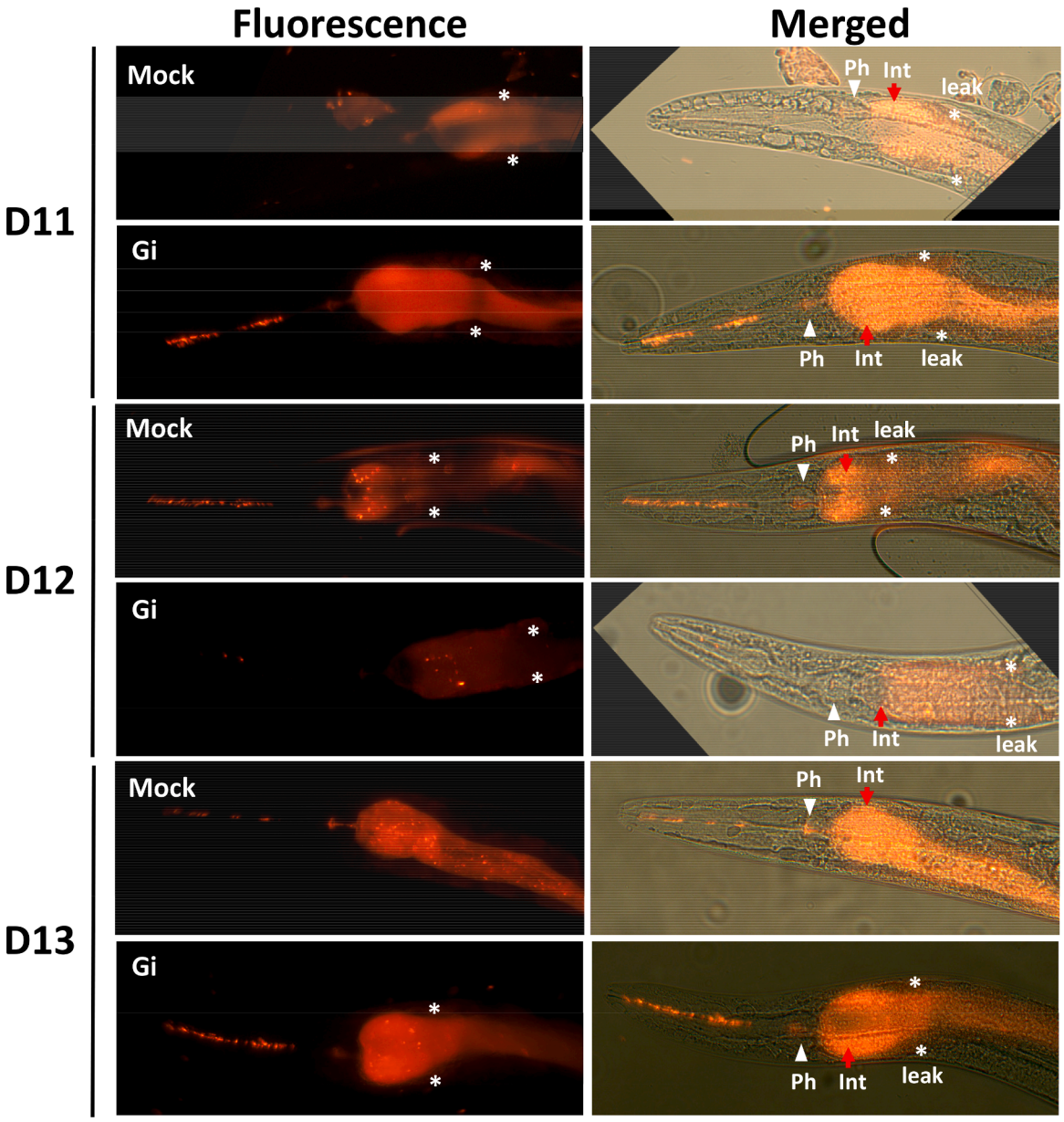

Fig. 2. (*continued*).

response (Fig. 3a and Table 1). A related process, the defense response to gram-negative bacteria, was also listed. This indicated that innate immunity is the most critical biological process modulated by *gspd-1* in *C. elegans*. qPCR was employed to validate the DEGs in the innate immune response. The expression level of selected DEGs was comparable with the RNAseq analysis (Fig. 3b).

3.3. Reduced tight junction gene expression in gspd-1-knockdown *C. elegans* and a G6PD-deficient human colon cell line

The RNAseq analysis revealed that among the DEGs in the innate immunity response, down-regulation of *clc-1* (0.43 fold) and *tsp-1* (0.15 fold) were detected in *gspd-1*-knockdown *C. elegans* (Table 1). To examine whether or not *gspd-1* deficiency affects the expression of TJ and immune-related genes in *C. elegans, zoo-1, clc-1, and tsp-1* were analyzed by qPCR. The transcript level of these genes was reduced in *gspd-1*-knockdown *C. elegans* (Fig. 4a). The down-regulation of *clc-1* and *zoo-1* indicates that *gspd-1* plays a role in the maintenance of barrier integrity of the digestive tract in *C. elegans*. The colon epithelium HCT116 cell line treated with G6PD inhibitors (6-AN and DHEA), was analyzed by qPCR to investigate whether or not G6PD deficiency modulates TJ genes in human cells. 6-AN treatment down-regulated *ZO-1* and *ATF-3*, while DHEA treatment down-regulated *ZO-1, ZO-2, Claudin-4* and *ATF-3* (Fig. 4b). The findings in the human colon cells were consistent with that of *C. elegans*, indicating that the modulation of the TJ genes by *G6PD* and *gspd-1* is conserved in humans and nematodes, respectively. During infection, KP down-regulated *clc-1* and *zoo-1* genes in *C. elegans*, while *gspd-1*-knockdown further down-regulated TJ genes compared to the Mock control at 2, 6, and 11 dpi (Fig. 5). Reduced expression of TJ genes upon infection with KP indicated that *gspd-1* deficiency is prone to severe tissue damage.

3.4. Genetic interaction of gspd-1 with daf-2 and down-stream effectors upon infection with KP

The survival and GSPD-1 activity of the *gspd-1*-knockdown *daf-2* mutant infected with KP was evaluated to understand the relationship between GSPD-1 and DAF-2 during bacterial pathogenesis (Fig. 6).

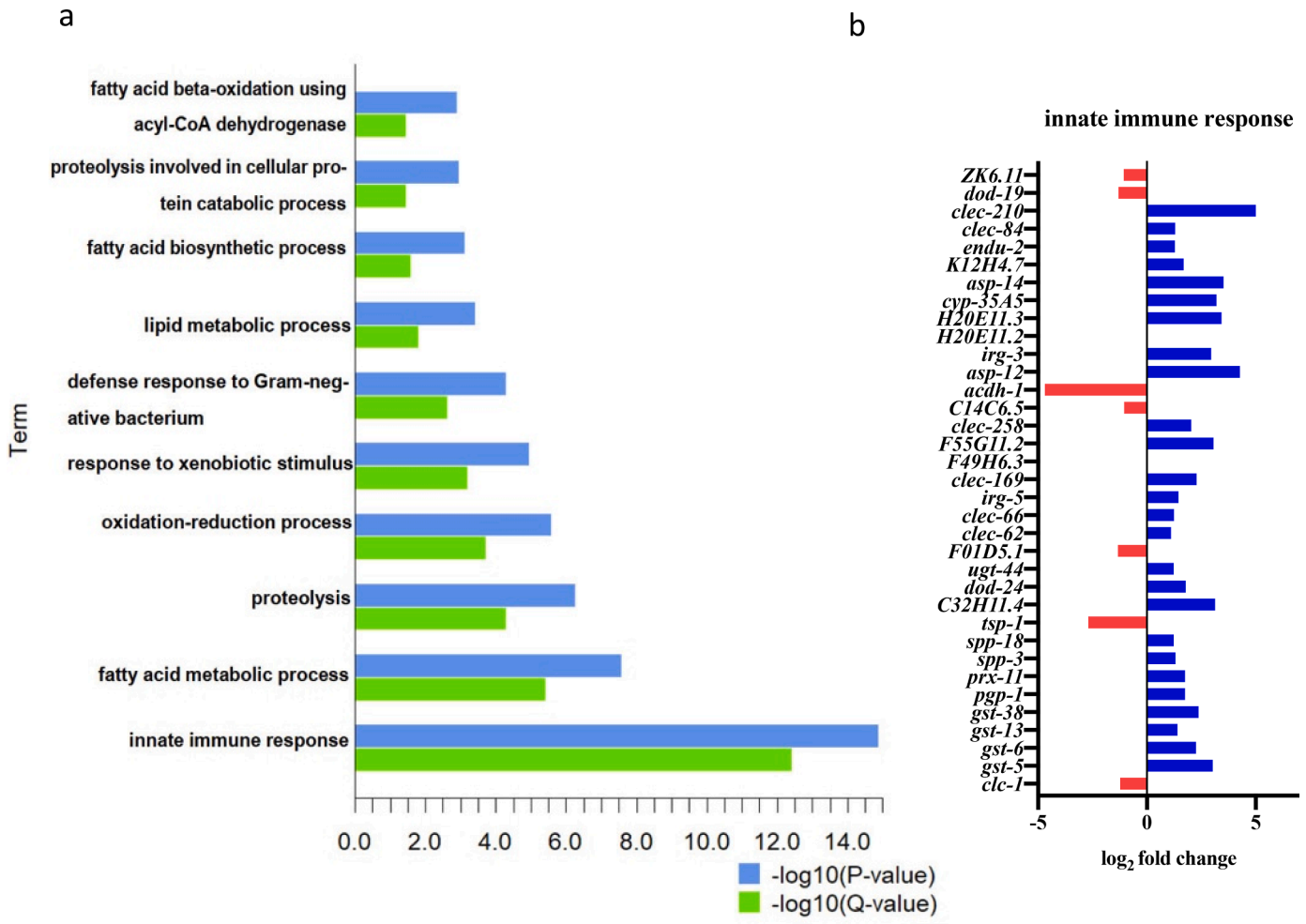

Fig. 3. RNAseq analysis of the Mock control and *gspd-1* (RNAi) *C. elegans*. (a) The top 10 enriched GO biological process terms were plotted on the y-axis versus a measure of significance (negative logarithm of the P-value or Q-value) on the x-axis. The Q-value was calculated by Benjamini. (b) The DEGs between the Mock control and *gspd-1* (RNAi) *C. elegans*.

Inactivation of *daf-2* restored the shorten lifespan caused by KP in *gspd-1*-knockdown *C. elegans* infected with KP (Fig. 6a). Likewise, KP-derived shorten lifespan in *gspd-1*-knockdown *C. elegans* was not observed in the *daf-16* mutant (Fig. 6b). *daf-2* mutation increased GSPD-1 activity in both basal condition (Fig. 6c) and *gspd-1* deficiency (Fig. 6d), indicating that DAF-2 acts up-stream of GSPD-1.

Under basal conditions, where *E. coli* was the food source, the transcript level of *lys-7* did not change between the Mock control and *gspd-1*-knockdown *C. elegans* (Fig. 7a). However, *lys-7* was reduced ($P<0.001$) as early as 2 days and up to 11 days in *gspd-1*-knockdown *C. elegans* infected with KP (Fig. 7b).

3 types of *lys* genes and 2 types of *ilys* genes were examined by qPCR to confirm whether or not the expression of *C. elegans* lysozymes was affected by *gspd-1*. At 2 or 3 dpi, all lysozyme genes were down-regulated in *gspd-1*-knockdown *C. elegans* infected with KP (Figure S3). The reduced *LYZ* (lysozyme) gene expression in HCT116 cells treated with G6PD inhibitors was consistent with that of C. elegans, suggesting that *G6PD/gspd-1* is required for the expression of lysozymes (Fig. 7c).

3.5. Role of daf-2 in gspd-1 knockdown C. elegans induced by KP

Upon infection with KP, *lys-7* expression continued to increase at 6 and 11 dpi compared with 2 dpi in the *daf-2* mutant. In *gspd-1*-knockdown, *lys-7* expression was suppressed compared to the *daf-2* mutant (Fig. 8). There was a down-hill trend of gene expression in the *daf-2* mutant, suggesting that *daf-2* inactivation is still sensitive to KP-induced TJ damage and immune dysfunction (Fig. 8). Gene expression in the double deficiency of *gspd-1* and *daf-2* did not differentiate that from the *daf-2* mutant (Fig. 8). This is consistent with the fact that the lifespan of the *gspd-1*-knockdown *daf-2* mutant was identical to that of the *daf-2* mutant (Fig. 6). Epigenetic analysis showed that deletion of *clc-1, tsp-1*, or *lys-7* abolished the lethality of *gspd-1*-deficient *C. elegans* infected with KP (Fig. 9), indicating that *clc-1, tsp-1*, and *lys-7* were down-stream targets of *gspd-1*, and involved in anti-microbial defense.

4. Discussion

Traditional G6PD studies mainly have focused on red cell-related pathology. *Plasmodium* infection causes hemolytic anemia in G6PD deficient individuals. *Clostridium difficile* infection precipitates hemolysis in G6PD-deficient premature neonates leading to severe neonatal jaundice (Kaplan et al., 2008). Neutrophil dysfunction and viral infection contribute to G6PD deficiency-induced cellular pathophysiology. The current study is the first report showing that G6PD deficiency is an immune-compromised risk factor in an animal model. Impaired immune effector lysozymes and TJ genes were found in GSPD-1-deficient *C. elegans* infected with KP. The dysregulated innate immunity and intestinal barrier dysfunction caused increased bacterial colonization and translocation, leading to a shorten lifespan.

Lack of G6PD is associated with an impaired immune response. LPS or PMA-stimulated nitric oxide, superoxide, and hydrogen peroxide are abrogated in G6PD-deficient granulocytes (Tsai et al., 1998).

Table 1
List of DEGs in the innate immune response.

GO:0,045,087~innate immune response; Q-value: 3.74367E-13						
Gene symbol	Description	Ensembl Gene ID	Fold change	log2 fold change	p value	q value
clc-1	CLaudin-like in Caenorhabditis [Source:UniProtKB/TrEMBL;Acc:Q93198]	WBGene00000522	0.4257	-1.231932653	0.04295	0.904228
gst-5	Probable glutathione S-transferase 5 [Source:UniProtKB/Swiss-Prot;Acc:Q09596]	WBGene00001753	8.1208	3.021614541	0.00005	0.0186075
gst-6	Probable glutathione S-transferase 6 [Source:UniProtKB/Swiss-Prot;Acc:P91252]	WBGene00001754	4.8036	2.264104877	0.00265	0.234262
gst-13	Glutathione S-Transferase [Source:UniProtKB/TrEMBL;Acc:Q22814]	WBGene00001761	2.6450	1.403288469	0.0105	0.464447
gst-38	Glutathione S-Transferase [Source:UniProtKB/TrEMBL;Acc:O45451]	WBGene00001786	5.2102	2.381347459	0.00545	0.339089
pgp-1	Multidrug resistance protein pgp-1 [Source:UniProtKB/Swiss-Prot;Acc:P34712]	WBGene00003995	3.3795	1.756796853	0.00135	0.167657
prx-11	PeRoXisome assembly factor [Source:UniProtKB/TrEMBL;Acc:O62103]	WBGene00004196	3.3645	1.750389138	0.04155	0.89061
spp-3	SaPosin-like Protein family [Source:UniProtKB/TrEMBL;Acc:Q22336]	WBGene00004988	2.4755	1.307696008	0.00555	0.341466
spp-18	SaPosin-like Protein family [Source:UniProtKB/TrEMBL;Acc:A0A061AKY5]	WBGene00005003	2.3583	1.237750421	0.0069	0.377793
tsp-1	Tetraspanin-1 [Source:UniProtKB/Swiss-Prot;Acc:P34285]	WBGene00006627	0.1542	-2.696842482	0.03025	0.757338
dod-24	Downstream Of DAF-16 (Regulated by DAF-16) [Source:UniProtKB/TrEMBL;Acc:Q9XUH3]	WBGene00007875	3.4515	1.787225622	0.00005	0.0186075
ugt-44	UDP-GlucuronosylTransferase [Source:UniProtKB/TrEMBL;Acc:O17757]	WBGene00008486	2.3475	1.23110459	0.0111	0.477571
clec-62	C-type LECtin [Source:UniProtKB/TrEMBL;Acc:O45441]	WBGene00009393	2.1624	1.112619742	0.0052	0.333147
clec-66	C-type LECtin [Source:UniProtKB/TrEMBL;Acc:O45445]	WBGene00009397	2.3773	1.249337185	0.01825	0.594303
irg-5	Infection Response protein [Source:UniProtKB/TrEMBL;Acc:O02357]	WBGene00009429	2.7378	1.453033477	0.02305	0.651854
clec-169	C-type LECtin [Source:UniProtKB/TrEMBL;Acc:A4F316]	WBGene00009526	4.8700	2.283912396	0.00945	0.445075
clec-258	C-type LECtin [Source:UniProtKB/TrEMBL;Acc:Q9XUC9]	WBGene00010928	4.1181	2.041973834	0.0366	0.833835
acdh-1	Acyl CoA DeHydrogenase [Source:UniProtKB/TrEMBL;Acc:Q8IAB6]	WBGene00016943	0.0388	-4.688114218	0.02425	0.667781
asp-12	ASpartyl Protease [Source:UniProtKB/TrEMBL;Acc:O01531]	WBGene00017678	19.3370	4.273292678	0.00005	0.0186075
irg-3	Infection Response protein [Source:UniProtKB/TrEMBL;Acc:A0A0M7RF66]	WBGene00018760	7.7878	2.961216301	0.00005	0.0186075
cyp-35A5	CYtochrome P450 family [Source:UniProtKB/TrEMBL;Acc:O44649]	WBGene00019473	9.2017	3.201892871	0.01645	0.56268
asp-14	ASpartyl Protease [Source:UniProtKB/TrEMBL;Acc:Q94271]	WBGene00019619	11.4504	3.517320461	0.0007	0.116195
K12H4.7	Putative serine protease K12H4.7 [Source:UniProtKB/Swiss-Prot;Acc:P34528]	WBGene00019682	3.2259	1.689708186	0.00005	0.0186075
endu-2	ENDonuclease, poly(U) specific [Source:UniProtKB/TrEMBL;Acc:Q9GYM9]	WBGene00019779	2.4527	1.294400091	0.0046	0.31666
clec-84	C-type LECtin [Source:UniProtKB/TrEMBL;Acc:Q8WTL2]	WBGene00021895	2.4709	1.305050903	0.01945	0.611471
clec-210	C-type LECtin [Source:UniProtKB/TrEMBL;Acc:Q9TXW7]	WBGene00022261	32.1417	5.006376442	0.00745	0.395024
dod-19	Downstream Of DAF-16 (Regulated by DAF-16) [Source:UniProtKB/TrEMBL;Acc:A0A0K3ASK2]	WBGene00022644	0.4043	-1.306647425	0.0007	0.116195

G6PD-deficient epithelial cells are sensitive to *Staphylococcus aureus* infection (Hsieh et al., 2013). Impaired inflammasome activation and bacterial clearance have been observed in G6PD-deficient peripheral blood mononuclear cells from patients and human monocytic THP-1 cells (Yen et al., 2020). These studies highlight an essential role of G6PD in the cellular immune response, however, a need for a comprehensive understanding of this biological process at the organismal level cannot be met without a proper animal model. A simple invertebrate organism, such as *C. elegans*, has become an attractive animal model for studying the mechanism of the innate immune response. In particular, it has facilitated the identification of new virulence factors, host immune pathways, and the mechanism of host-pathogen interactions. Despite the evolutionary distance between *C. elegans* and humans, their host-pathogen interactions are surprisingly similar (Ermolaeva and Schumacher, 2014). Hence, it is a valuable tool for elucidating host-pathogen interactions and identifying the link between modulators and effectors. Such mechanistic studies can also shed light on the discovery of potential anti-microbial strategies.

C. elegans as a model has been used for the study of common human intestinal pathogens, including *P. aeruginosa* and *S. typhimurium* (Tan and Ausubel, 2000; Vega et al., 2013). Short-term infection with KP in *C. elegans* causes a distended intestine and intestinal atrophy (Kamaladevi and Balamurugan, 2017). Proteomic analysis reveals that infection with KP in *C. elegans* induces autophagy due to inhibition of mTOR, resulting in dauer formation. In the current study, long-term KP infection was consistent with previous findings that KP infection mainly disrupts intestinal physiology. GSPD-1 deficiency is prone to increasing the KP burden, as colonization is an essential strategy in bacterial pathogenesis. Unregulated intestinal bacterial proliferation or dysbiosis reduces *C. elegans* lifespan (Portal-Celhay et al., 2012). Extensive

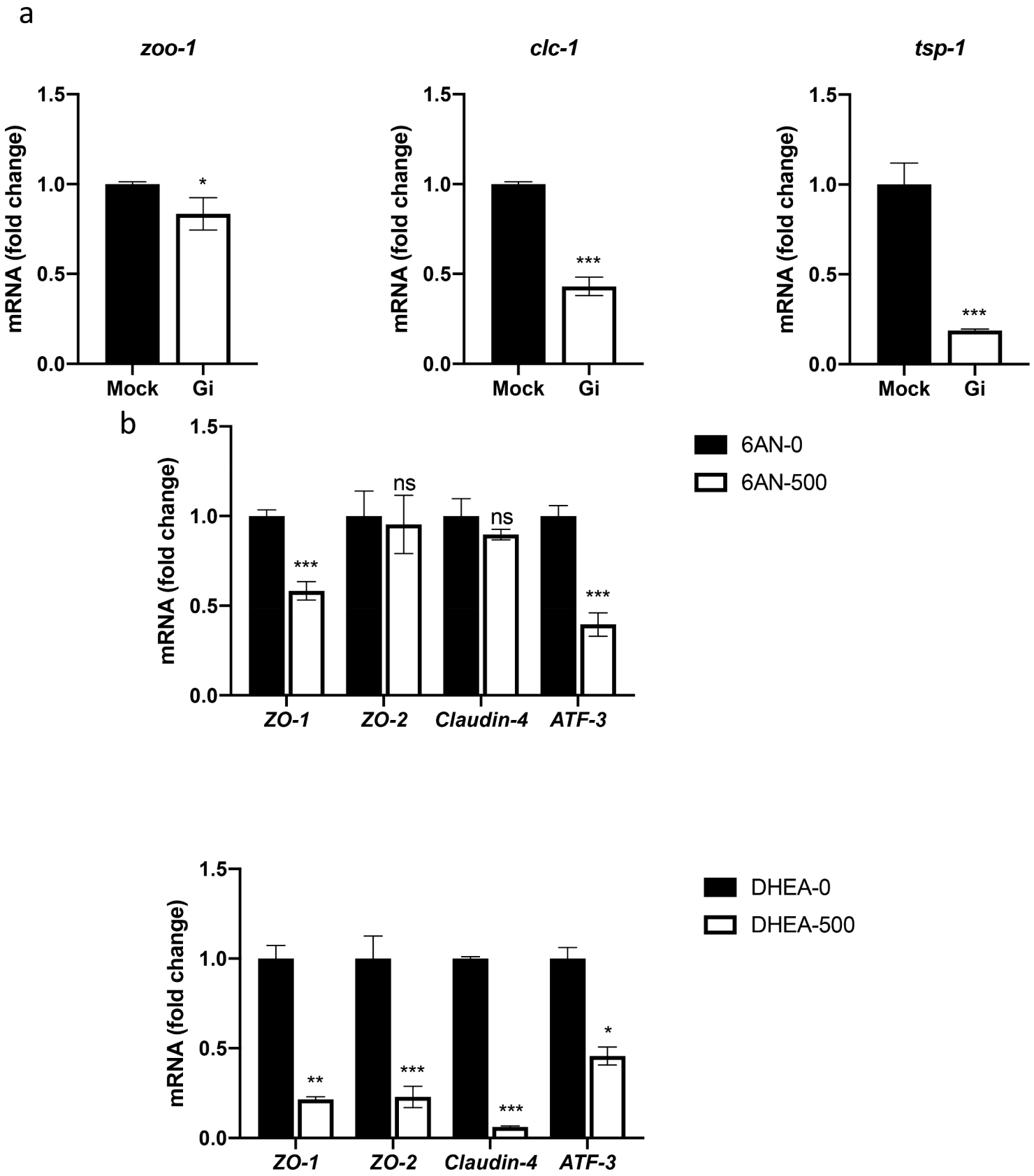

Fig. 4. Gene expression of TJ and the innate immune response. (a) the Mock control and *gspd-1* (RNAi) *C. elegans*, (b) human colon epithelial HCT116 cells with and without the G6PD inhibitor. Bars represents the mean±SD. *$P<0.05$; ***$P<0.001$.

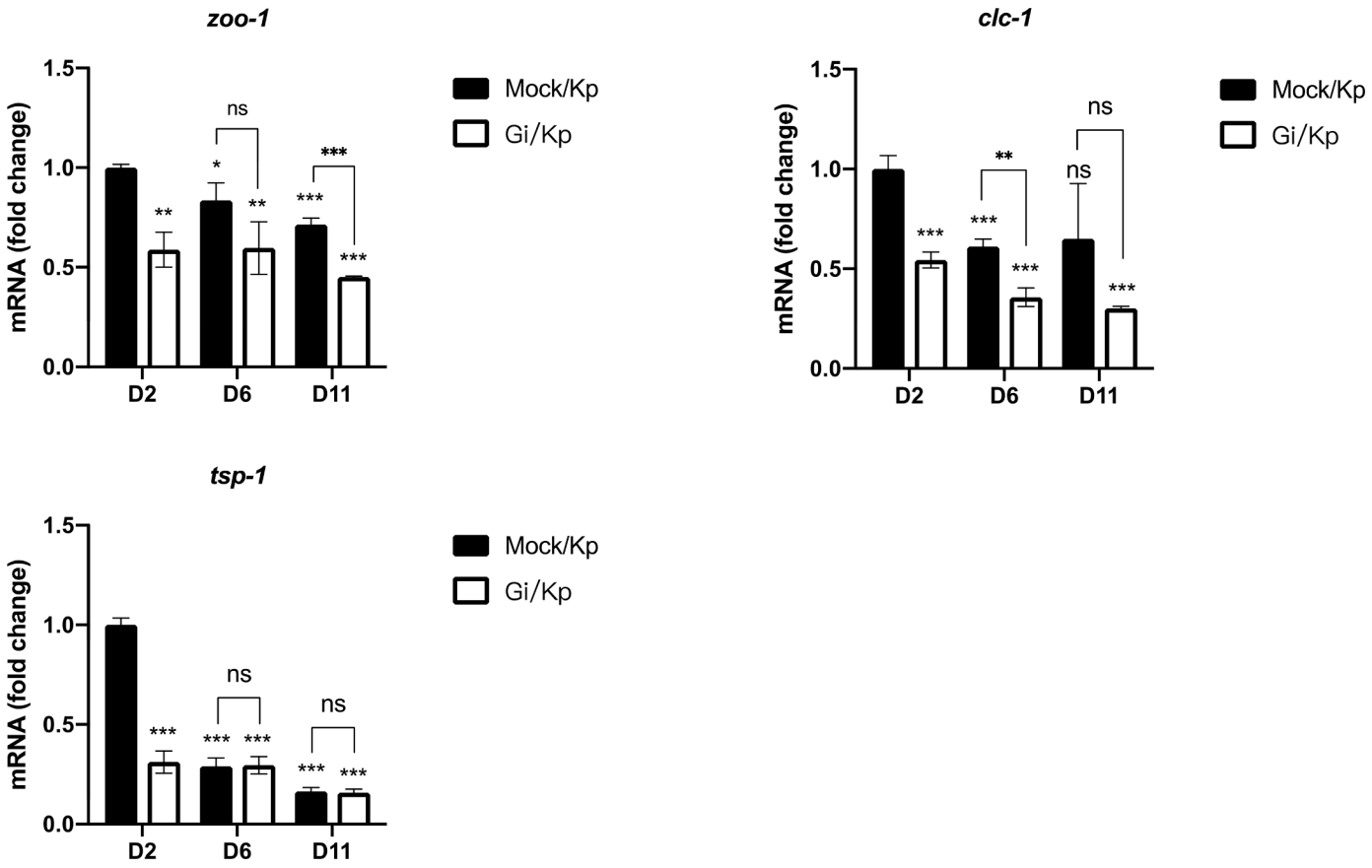

Fig. 5. Gene expression of TJ and the innate immune response of the Mock control and *gspd-1* (RNAi) *C. elegans* infected with KP. Bars represents the mean±SD. **P*<0.05; ***P*<0.01, ****P*<0.001.

bacterial colonization is consistent with the increased lethality caused by KP, indicating that an immune-compromised condition induced by GSPD-1 deficiency increases disease severity.

RNAseq is a powerful platform for screening differential gene expression under genetic manipulation. Transcriptomic analysis by RNAseq revealed several "downstream targets of DAF-16″ (*dod*) genes in the innate immune response, suggesting that *daf-16* is involved in the *gspd-1*-mediated innate immune response. Inactivation of the insulin/IGF-1 signaling (IIS) pathway during adulthood enhances *C. elegans* lifespan and innate immunity (Garsin et al., 2003). Mutation of *daf-2* is associated with reduced colonization and enhanced clearance of bacterial pathogens in *C. elegans* (EA Evans et al., 2008). DAF-16, the forkhead box O (FOXO) transcription factor, is activated in the absence of DAF-2. Nuclear translocation of DAF-16 triggers gene expression, including longevity and the stress response. A proteomic study in *C. elegans* has revealed that several glycolytic enzymes, including GSPD-1, are up-regulated in *daf-2* mutants (Depuydt et al., 2014). Since G6PD is associated with the cellular immune response against human bacterial pathogens (Yen et al., 2020; Hsieh et al., 2013), GSPD-1 may directly or indirectly interact with the IIS pathway and contribute to cellular anti-microbial defense.

Transcriptional profiling has identified target genes whose expression is up-regulated by DAF-16 and DAF-2 either directly or indirectly, for example, antimicrobial effector molecules, such as lysozymes (EA Evans et al., 2008). Resistance to bacterial infections is associated with increased immunity gene expression in *daf-2* mutant (EA Evans et al., 2008). *lys-7* expressed in the *C. elegans* intestine, is necessary for restricting bacteria colonization in the *daf-2* mutant (EA Evans et al., 2008). Phylogenetic sequence analysis has revealed that 16 lysozymes with varied sequence divergence are found in *C. elegans* (Schulenburg and Boehnisch, 2008). One class is related to protists (*lys*) and the other belongs to invertebrate types (*ilys*). *Pseudomonas aeruginosa* inhibits the *C. elegans* immune response by down-regulating *lys-7*, while *lys-7* expression is restored in the *daf-2* mutant (EA Evans et al., 2008; Fatin et al., 2017). *lys-7* was increased in the *daf-2* mutant, while *lys-7* expression was suppressed in *gspd-1*-deficient *C. elegans* infected with KP. These findings indicate that the modulation of lysozymes is critical in host-pathogen interactions. Even so, the attenuated expression of lysozymes in GSPD-1 deficiency was not reflected in the lifespan assay. Perhaps an alternative pathway under *daf-2* inactivation plays an important role in pathogen defense and the maintenance of organismal survival.

GSPD-1 is required during reproduction and embryonic development (Yang et al., 2020; Yang et al., 2013). Although GSPD-1 deficiency does not affect growth during neither the larval stage nor the lifespan in adults, GSPD-1 knockdown at the larval stage results in enhanced germ cell apoptosis and embryonic pathologies. Reduced GSPD-1 activity at the larval stage is sufficient to alter the innate immune response and induce long-term pathologies upon pathogenic infection, suggesting that a temporal requirement of GSPD-1 activity is involved in the immune response.

During embryonic development, one of the main embryonic pathologies in GSPD-1-deficient embryos is the disruption of the permeability barrier in the egg shell, which causes increased permeability and embryonic lethality (Chen et al., 2017). Among the DEGs in the innate immune response, *clc-1* is a TJ gene. *clc-1* (Claudin-like in Caenorhabditis), the orthologue of human claudin, is involved in epithelial cell-cell adhesion and anti-bacterial defense (Asano et al., 2003). The barrier integrity of the pharynx requires CLC-1. Knockdown of *clc-1* causes dextran diffusion to the outside of the lumen of the digestive tract, indicating a disruption of barrier function in the pharyngeal portion of the intestine (Asano et al., 2003). *tsp-1* encodes a tetraspanin

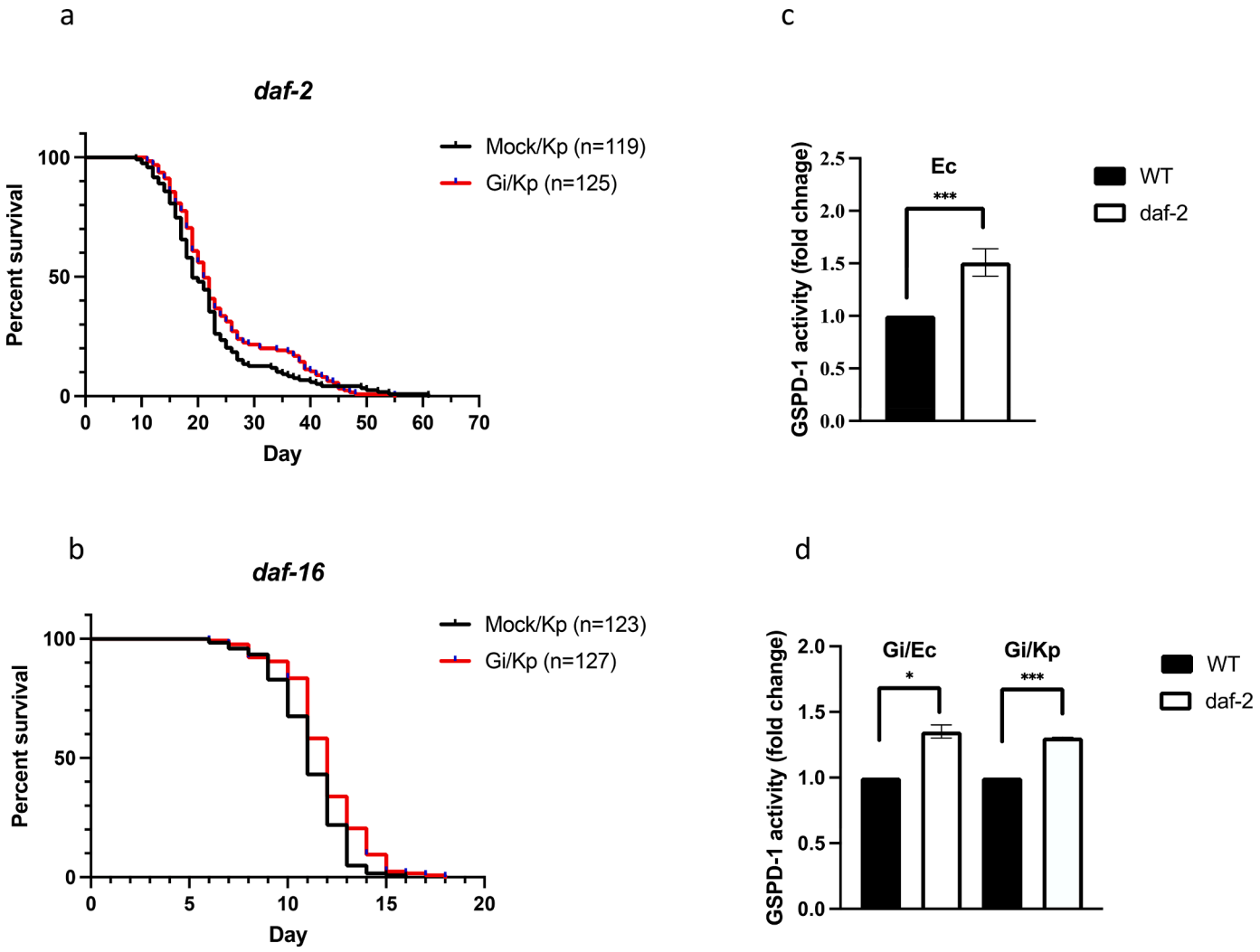

Fig. 6. Survival and GSPD-1 status of the *gspd-1* and IIS signaling mutant background infected with KP. (a) Lifespan of the Mock control and *gspd-1* (RNAi) *C. elegans* in the *daf-2* mutant, (b) Lifespan of the Mock control and *gspd-1* (RNAi) *C. elegans* in the *daf-16* mutant. (c) GSPD-1 activity with OP50. (d) GSPD-1 activity with HT115 and KP. Bars represents the mean±SD. *$P<0.05$; ***$P<0.001$.

and is involved in the pathogen response in *C. elegans* (Kudlow et al., 2012). ZO-1, a biomarker of disrupted barrier function in humans, is involved in the regulation of intestinal TJ permeability (Power et al., 2021). *zoo-1*, an orthologue of zonula occluden (ZO-1), is located in the adherens junction and the bi-cellular TJ in *C. elegans*. As defective TJ in *C. elegans* contributed to the bacterial virulence, remodeling and repair of TJ is important for preventing microbial pathogenesis (Gonzalez et al., 2009). It is hypothesized that increased sensitivity to pathogen-derived toxins, instead of dissemination of bacteria across the intestine, is capable of increasing bacteria susceptibility in *C. elegans* (Sim and Hibberd, 2016). Consistent with the dysfunctional embryonic barrier, altered TJ expression was associated with GSPD-1 deficiency. These findings suggest that G6PD activity is tightly connected to membrane integrity and function. Transketolase (TKT), the key enzyme in the non-oxidative branch of the PPP, is closely associated with inflammatory bowel disease (IBD) (Tian et al., 2021). The mouse model lacking TKT in intestinal epithelial cells shows growth retardation and colitis. Specifically, TKT deficiency causes mucosal erosion, impaired TJ and barrier function, and elevated inflammatory cell penetration, indicating that the PPP is required for barrier function. Ablation of key enzymes in the PPP can lead to severe immune dysfunction in the digestive tract.

Translocation of bacteria or bacterial components across intestinal cells can be achieved through different pathways (Martel et al., 2022). For example, bacterial lipopolysaccharides (LPS) and microbe-associated molecular patterns (MAMPs) can be taken up by endocytosis via a trans-cellular pathway. Bacteria and MAMPs can also be absorbed through a paracellular pathway by immune cells and TJ rearrangement. Unrestricted passage of pathogens can occur in the presence of ulcers, erosion or intestinal cell death. The localization of KP outside the foregut (pharynx) was observed in *C. elegans* infected with KP, indicating a leak. Active bacterial invasion through the transcellular pathway contributes to the intestinal translocation of KP in human enterocyte-like cell lines (Hsu et al., 2015).

The RNAseq analysis showed that *tsp-1* is a target of *gspd-1*. Tetraspanin is a protein family that serves as an organizer or scaffold for other proteins (Perot and Menager, 2020). TSP-15 is required for the activation of BLI-3 (Dual Oxidase) coupled with the dual oxidase maturation factor (DUOXA). Deficiency of BLI-3, DUOXA and peroxidase MLT-7 phenocopies the exoskeletal defect of the *tsp-15* mutant in *C. elegans*. The protein complex formed by TSP-15, BLI-3, and DOXA-1 is required for ROS production and for the cross-linking of collagen during cuticle synthesis (Moribe et al., 2012). *C. elegans* produces ROS when infected with *Entercoccus faecalis* infection, however, knockdown of *bli-3* in the intestine and hypodermis reduces ROS production, leading to increased susceptibility to *E. faecalis* (Chavez et al., 2009).

NADPH oxidase 1 (NOX1)-deficient mice display low levels of ROS production in the intestine, a mucus layer defect with bacterial infiltration into crypts and susceptibility to colitis, leading to mortality

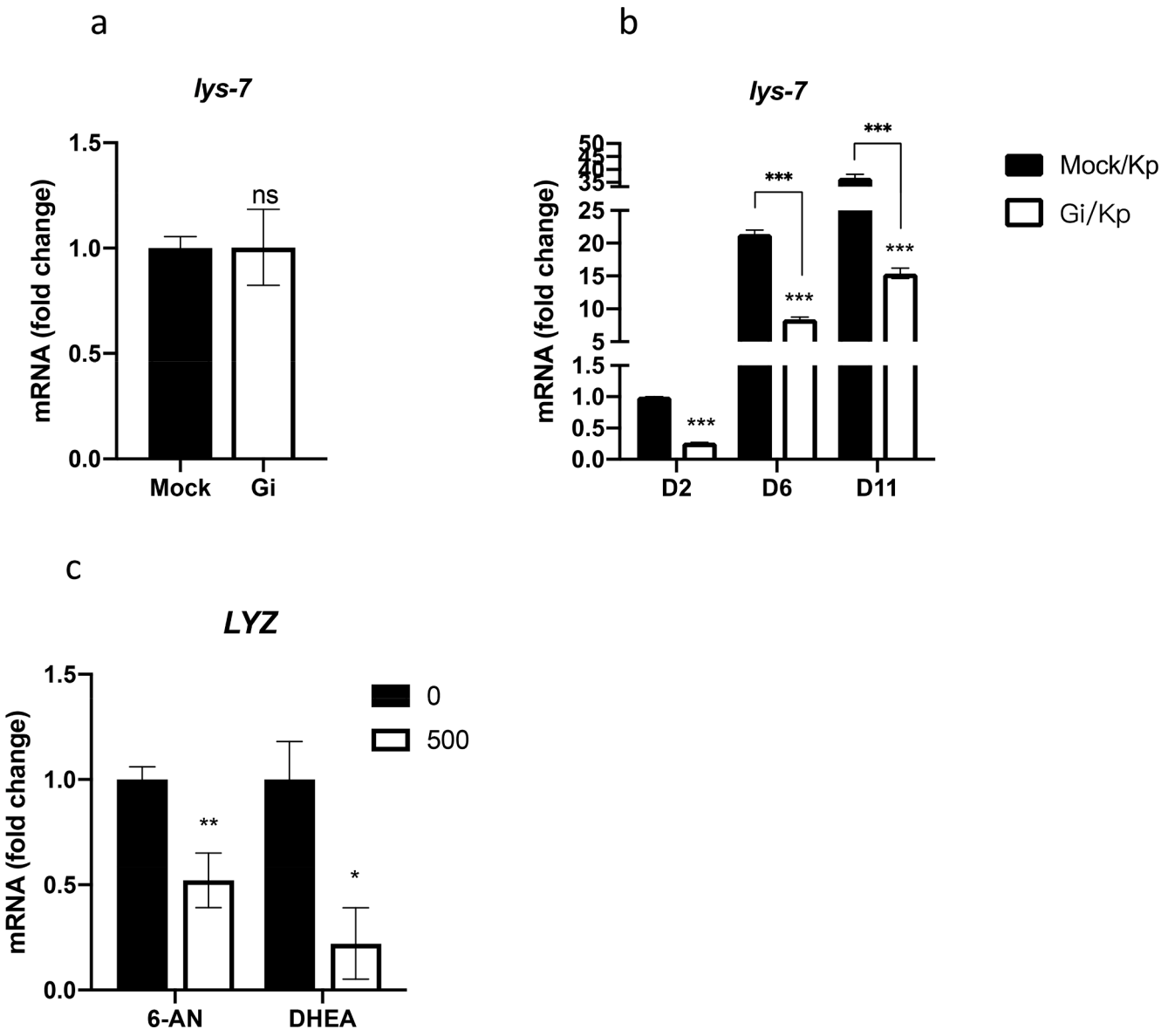

Fig. 7. Gene expression of lysozymes in *C. elegans* and a human cell line HCT116. (a) the Mock control and *gspd-1* (RNAi) *C. elegans* without KP. (b) the Mock control and *gspd-1* (RNAi) *C. elegans* infected with KP. (c) HCT116 cell treated with G6PD inhibitors. Bars represents the mean±SD. *$P<0.05$; **$P<0.01$, ***$P<0.001$.

(Aviello et al., 2019). In addition to causing colon damage, NOX variants induce IBD (Makhezer et al., 2019; Hayes et al., 2015; Dhillon et al., 2014). The colitis observed in IBD is similar to chronic granulomatous disease (CGD), which is an immunodeficiency due to defective NOX (Dhillon et al., 2014). Clinical studies indicate that severe or complete deficiency of G6PD activity is associated with neutrophil dysfunction, including low H_2O_2 production and inefficient bactericidal activity, resembling CGD (Vives Corrons et al., 1982; Cooper et al., 1972; Baehner et al., 1972; Gray et al., 1973). Since NOX activity is determined by the availability of NADPH, G6PD is indispensable for NOX because G6PD is the major source for NADPH in the cell. Reduction of H_2O_2-derived from NOX is detected in G6PD-deficient granulocytes (Tsai et al., 1998). In addition to the intestine and hypodermis, BLI-3 also localizes in the pharynx (van der Hoeven et al., 2015). The alteration of *clc-1, tsp-1,* and *lys-7* in GSPD-1-deficient *C. elegans* infected with KP indicates that GSPD-1 is a master regulator in the anti-microbial defense (Fig. 10).

In conclusion, GSPD-1 maintains barrier integrity and boosts immunity through maintaining barrier junction and lysozymal activity in the intestine. In GSPD-1-deficient *C. elegans* infected with KP, an impaired tight junction rendered translocation of bacteria and/or toxins, while defective bacteriolytic ability failed to restrict bacterial colonization, leading to their demise.

Funding

This work is supported by a grant from the Ministry of Science and Technology of Taiwan (MOST-109-2320-B-264-001-MY2 to HCY). Supports also from En Chu Kong Hospital (106-COMP6012-10 to HCY and D02-03-005-03 to JHC)

CRediT authorship contribution statement

Wan-Hua Yang: Investigation, Validation. **Po-Hsiang Chen:** Investigation, Validation. **Hung-Hsin Chang:** Investigation, Software, Visualization. **Hong Luen Kwok:** Investigation, Software, Visualization. **Arnold Stern:** Writing – review & editing. **Po-Chi Soo:** Investigation, Methodology. **Jiun-Han Chen:** Conceptualization, Supervision. **Hung-Chi Yang:** Conceptualization, Writing – review & editing.

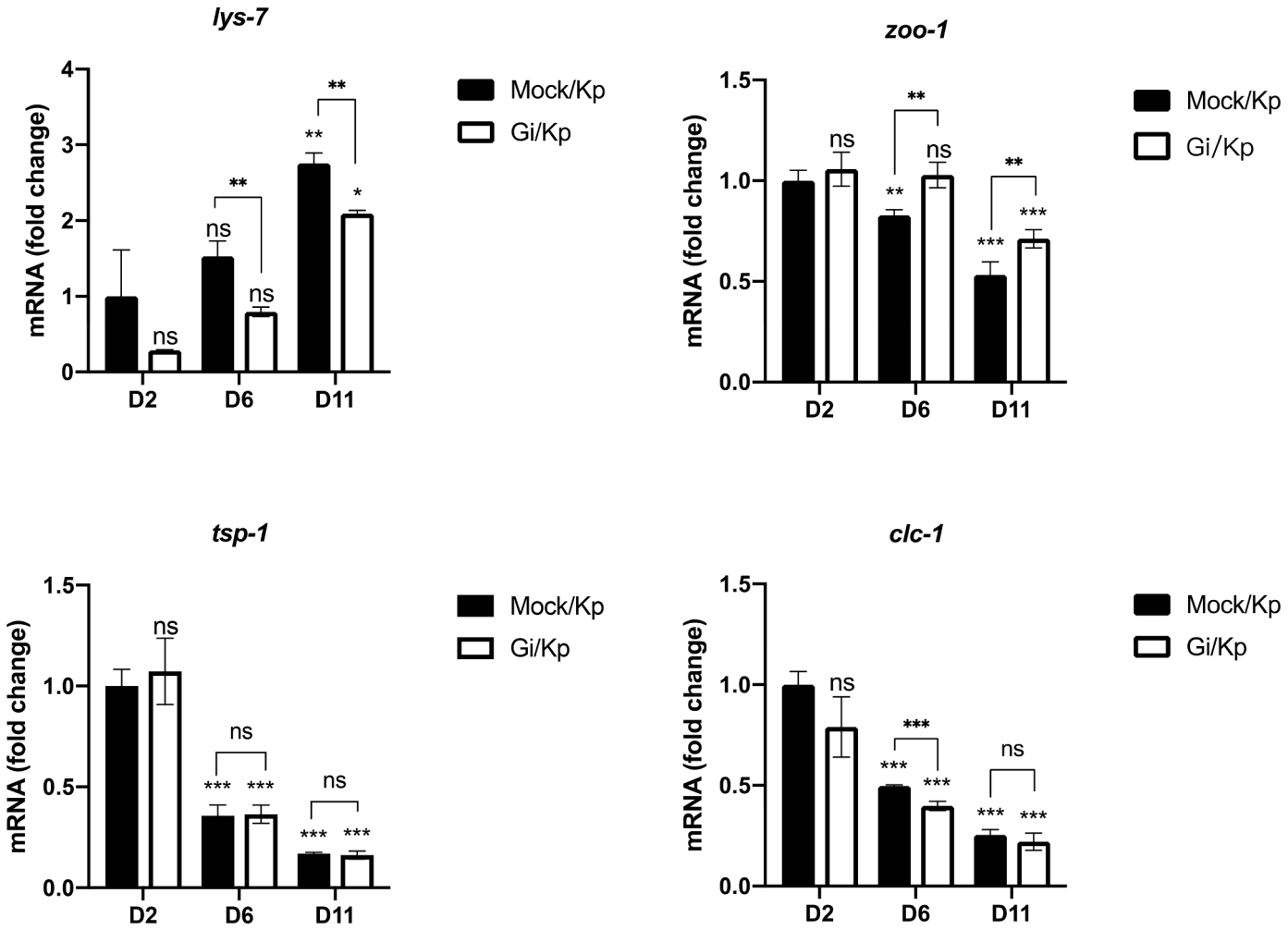

Fig. 8. Gene expression of lysozymes and TJ in the Mock control and *gspd-1* (RNAi) *daf-2* mutant *C. elegans* infected with KP. Bars represents the mean±SD. **P*<0.05; ***P*<0.01, ****P*<0.001.

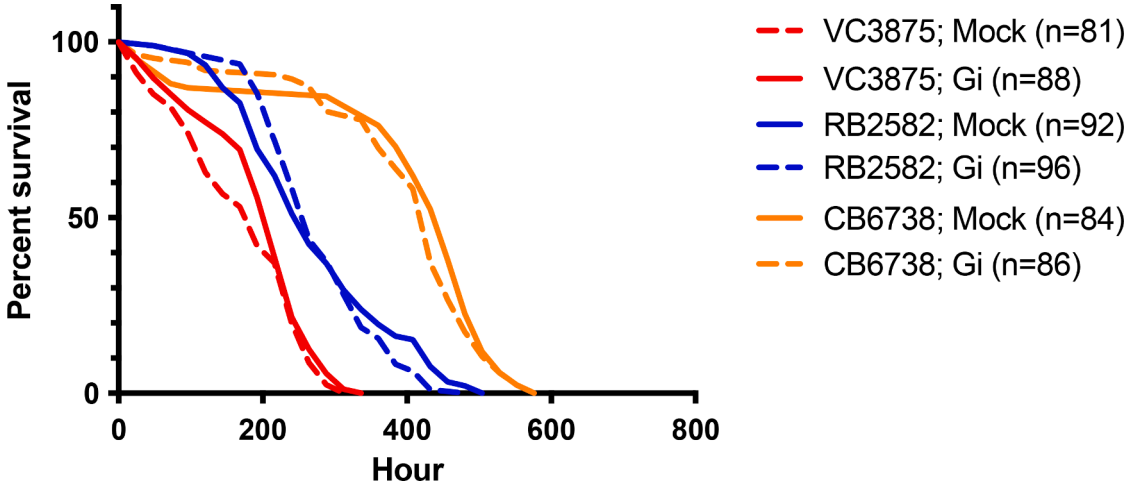

Fig. 9. Lifespan of the Mock control and *gspd-1* (RNAi) *clc-1, tsp-1* and *lys-7* mutant *C. elegans* infected with KP.

Declaration of Competing Interest

The authors declare the following financial interests/personal relationships which may be considered as potential competing interests:

Hung-Chi Yang reports financial support was provided by Ministry of Science and Technology of Taiwan. Hung-Chi Yang reports financial support was provided by En Chu Kong Hospital. Jiun-Han Chen reports financial support was provided by En Chu Kong Hospital. The corresponding author has served in the Editorial Board of "Current Research in Microbial Sciences".

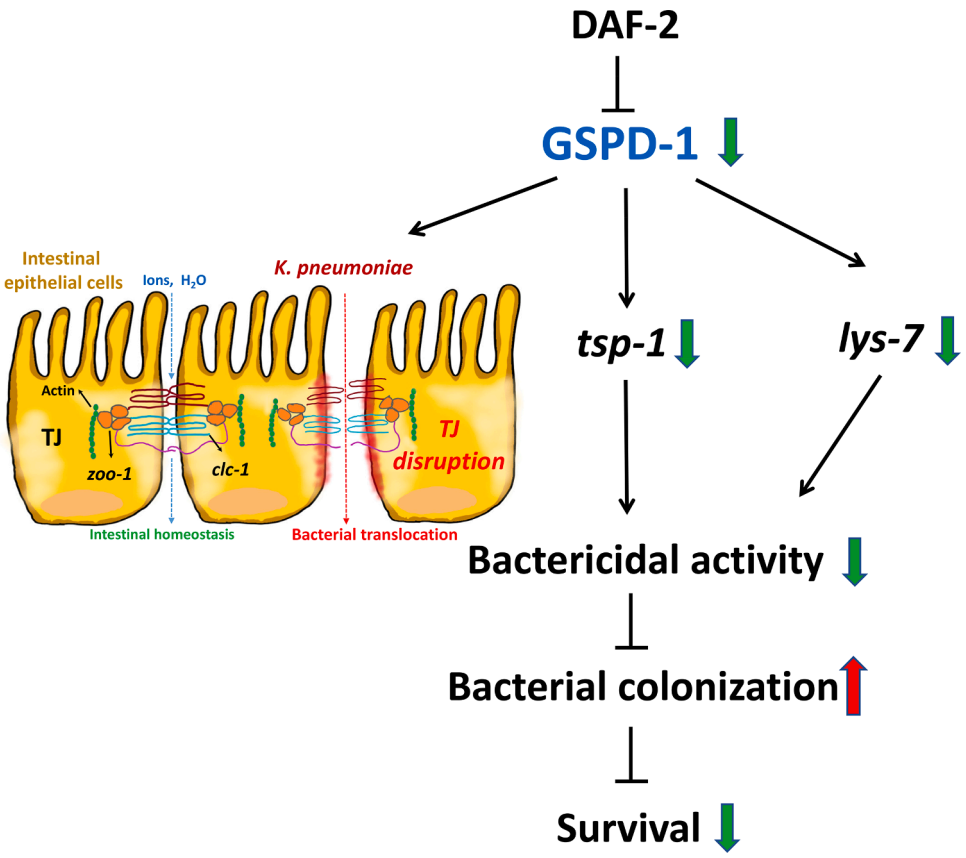

Fig. 10. Schematic diagram of how GSPD-1 status modulates innate immunity and survival in *C. elegans* infected with KP through the maintenance of barrier function (*clc-1* and *zoo-1*), innate immunity (*tsp-1*), and anti-microbial peptides (*lys-7*).

Data availability

Data will be made available on request.

Supplementary materials

Supplementary material associated with this article can be found, in the online version, at doi:10.1016/j.crmicr.2023.100181.

References

Asano, A., Asano, K., Sasaki, H., Furuse, M., Tsukita, S., 2003. Claudins in Caenorhabditis elegans: their distribution and barrier function in the epithelium. Curr. Biol. 13, 1042–1046.

Aviello, G., Singh, A.K., O'Neill, S., Conroy, E., Gallagher, W., D'Agostino, G., Walker, A. W., Bourke, B., Scholz, D., Knaus, U.G., 2019. Colitis susceptibility in mice with reactive oxygen species deficiency is mediated by mucus barrier and immune defense defects. Mucosal Immunol. 12, 1316–1326.

Ayala, F.R., Cogliati, S., Bauman, C., Lenini, C., Bartolini, M., Villalba, J.M., Arganaraz, F., Grau, R., 2017. Culturing bacteria from caenorhabditis elegans gut to assess colonization proficiency. Bio. Protoc. 7, e2345.

Baehner, R.L., Johnston Jr., R.B., Nathan, D.G., 1972. Comparative study of the metabolic and bactericidal characteristics of severely glucose-6-phosphate dehydrogenase-deficient polymorphonuclear leukocytes and leukocytes from children with chronic granulomatous disease. J. Reticuloendothel. Soc. 12, 150–169.

Chavez, V., Mohri-Shiomi, A., Garsin, D.A., 2009. Ce-Duox1/BLI-3 generates reactive oxygen species as a protective innate immune mechanism in Caenorhabditis elegans. Infect. Immun. 77, 4983–4989.

Chen, T.L., Yang, H.C., Hung, C.Y., Ou, M.H., Pan, Y.Y., Cheng, M.L., Stern, A., Lo, S.J., Chiu, D.T., 2017. Impaired embryonic development in glucose-6-phosphate dehydrogenase-deficient Caenorhabditis elegans due to abnormal redox homeostasis induced activation of calcium-independent phospholipase and alteration of glycerophospholipid metabolism. Cell Death. Dis. 8, e2545.

Cooper, M.R., DeChatelet, L.R., McCall, C.E., LaVia, M.F., Spurr, C.L., Baehner, R.L., 1972. Complete deficiency of leukocyte glucose-6-phosphate dehydrogenase with defective bactericidal activity. J. Clin. Invest. 51, 769–778.

Depuydt, G., Xie, F., Petyuk, V.A., Smolders, A., Brewer, H.M., Camp 2nd, D.G., Smith, R. D., Braeckman, B.P., 2014. LC-MS proteomics analysis of the insulin/IGF-1-deficient Caenorhabditis elegans daf-2(e1370) mutant reveals extensive restructuring of intermediary metabolism. J. Proteome Res. 13, 1938–1956.

Dhillon, S.S., Fattouh, R., Elkadri, A., Xu, W., Murchie, R., Walters, T., Guo, C., Mack, D., Huynh, H.Q., Baksh, S., et al., 2014. Variants in nicotinamide adenine dinucleotide phosphate oxidase complex components determine susceptibility to very early onset inflammatory bowel disease. Gastroenterology 147, 680–689 e682.

Ermolaeva, M.A., Schumacher, B., 2014. Insights from the worm: the C. elegans model for innate immunity. Semin. Immunol. 26, 303–309.

Evans, E.A., Chen, W.C., Tan, M.W., 2008a. The DAF-2 insulin-like signaling pathway independently regulates aging and immunity in C. elegans. Aging Cell 7, 879–893.

Evans, E.A., Kawli, T., Tan, M.W., 2008b. Pseudomonas aeruginosa suppresses host immunity by activating the DAF-2 insulin-like signaling pathway in Caenorhabditis elegans. PLoS Pathog. 4, e1000175.

Fatin, S.N., Boon-Khai, T., Shu-Chien, A.C., Khairuddean, M., Al-Ashraf Abdullah, A., 2017. A marine actinomycete rescues caenorhabditis elegans from pseudomonas aeruginosa infection through restitution of lysozyme 7. Front. Microbiol. 8, 2267.

Garsin, D.A., Villanueva, J.M., Begun, J., Kim, D.H., Sifri, C.D., Calderwood, S.B., Ruvkun, G., Ausubel, F.M., 2003. Long-lived C. elegans daf-2 mutants are resistant to bacterial pathogens. Science 300, 1921.

Gonzalez, J.E., DiGeronimo, R.J., Arthur, D.E., King, J.M., 2009. Remodeling of the tight junction during recovery from exposure to hydrogen peroxide in kidney epithelial cells. Free Radic. Biol. Med. 47, 1561–1569.

Gray, G.R., Stamatoyannopoulos, G., Naiman, S.C., Kliman, M.R., Klebanoff, S.J., Austin, T., Yoshida, A., Robinson, G.C., 1973. Neutrophil dysfunction, chronic granulomatous disease, and non-spherocytic haemolytic anaemia caused by complete deficiency of glucose-6-phosphate dehydrogenase. Lancet 2, 530–534.

Hayes, P., Dhillon, S., O'Neill, K., Thoeni, C., Hui, K.Y., Elkadri, A., Guo, C.H., Kovacic, L., Aviello, G., Alvarez, L.A., et al., 2015. Defects in NADPH oxidase genes NOX1 and DUOX2 in very early onset inflammatory bowel disease. Cell Mol. Gastroenterol. Hepatol. 1, 489–502.

Hsieh, Y.T., Lin, M.H., Ho, H.Y., Chen, L.C., Chen, C.C., Shu, J.C., 2013. Glucose-6-phosphate dehydrogenase (G6PD)-deficient epithelial cells are less tolerant to infection by Staphylococcus aureus. PLoS ONE 8, e79566.

Hsu, C.R., Pan, Y.J., Liu, J.Y., Chen, C.T., Lin, T.L., Wang, J.T., 2015. Klebsiella pneumoniae translocates across the intestinal epithelium via Rho GTPase- and phosphatidylinositol 3-kinase/Akt-dependent cell invasion. Infect. Immun. 83, 769–779.

Jorgensen, E.M., Mango, S.E., 2002. The art and design of genetic screens: caenorhabditis elegans. Nat. Rev. Genet. 3, 356–369.

Kamaladevi, A., Balamurugan, K., 2017. Global proteomics revealed klebsiella pneumoniae induced autophagy and oxidative stress in caenorhabditis elegans by inhibiting PI3K/AKT/mTOR pathway during infection. Front. Cell Infect. Microbiol. 7, 393.
Kaplan, M., Hammerman, C., Vreman, H.J., Wong, R.J., Stevenson, D.K., 2008. Severe hemolysis with normal blood count in a glucose-6-phosphate dehydrogenase deficient neonate. J. Perinatol. 28, 306–309.
Kudlow, B.A., Zhang, L., Han, M., 2012. Systematic analysis of tissue-restricted miRISCs reveals a broad role for microRNAs in suppressing basal activity of the C. elegans pathogen response. Mol. Cell 46, 530–541.
Luzzatto, L., Seneca, E., 2014. G6PD deficiency: a classic example of pharmacogenetics with on-going clinical implications. Br. J. Haematol. 164, 469–480.
Makhezer, N., Ben Khemis, M., Liu, D., Khichane, Y., Marzaioli, V., Tlili, A., Mojallali, M., Pintard, C., Letteron, P., Hurtado-Nedelec, M., et al., 2019. NOX1-derived ROS drive the expression of Lipocalin-2 in colonic epithelial cells in inflammatory conditions. Mucosal Immunol. 12, 117–131.
Martel, J., Chang, S.H., Ko, Y.F., Hwang, T.L., Young, J.D., Ojcius, D.M., 2022. Gut barrier disruption and chronic disease. Trends Endocrinol. Metab. 33, 247–265.
Moribe, H., Konakawa, R., Koga, D., Ushiki, T., Nakamura, K., Mekada, E., 2012. Tetraspanin is required for generation of reactive oxygen species by the dual oxidase system in Caenorhabditis elegans. PLos Genet. 8, e1002957.
Paczosa, M.K., Mecsas, J., 2016. Klebsiella pneumoniae: going on the offense with a strong defense. Microbiol. Mol. Biol. Rev. 80, 629–661.
Panjaitan, N.S.D., Horng, Y.T., Chien, C.C., Yang, H.C., You, R.I., Soo, P.C., 2021. The PTS components in Klebsiella pneumoniae affect bacterial capsular polysaccharide production and macrophage phagocytosis resistance. Microorganisms 9.
Perot, B.P., Menager, M.M., 2020. Tetraspanin 7 and its closest paralog tetraspanin 6: membrane organizers with key functions in brain development, viral infection, innate immunity, diabetes and cancer. Med. Microbiol. Immunol. 209, 427–436.
Portal-Celhay, C., Bradley, E.R., Blaser, M.J., 2012. Control of intestinal bacterial proliferation in regulation of lifespan in Caenorhabditis elegans. BMC Microbiol. 12, 49.
Power, N., Turpin, W., Espin-Garcia, O., Smith, M.I., Consortium, C.G.P.R., Croitoru, K., 2021. Serum zonulin measured by commercial kit fails to correlate with physiologic measures of altered gut permeability in first degree relatives of crohn's disease patients. Front. Physiol. 12, 645303.
Schulenburg, H., Boehnisch, C., 2008. Diversification and adaptive sequence evolution of Caenorhabditis lysozymes (Nematoda: rhabditidae). BMC Evol. Biol. 8, 114.
Sim, S., Hibberd, M.L., 2016. Caenorhabditis elegans susceptibility to gut Enterococcus faecalis infection is associated with fat metabolism and epithelial junction integrity. BMC Microbiol. 16, 6.
Stiernagle, T., 2006. Maintenance of C. elegans. WormBook 1–11.
Tan, M.W., Ausubel, F.M., 2000. Caenorhabditis elegans: a model genetic host to study Pseudomonas aeruginosa pathogenesis. Curr. Opin. Microbiol. 3, 29–34.
Tian, N., Hu, L., Lu, Y., Tong, L., Feng, M., Liu, Q., Li, Y., Zhu, Y., Wu, L., Ji, Y., et al., 2021. TKT maintains intestinal ATP production and inhibits apoptosis-induced colitis. Cell Death. Dis. 12, 853.
Tsai, K.J., Hung, I.J., Chow, C.K., Stern, A., Chao, S.S., Chiu, D.T., 1998. Impaired production of nitric oxide, superoxide, and hydrogen peroxide in glucose 6-phosphate-dehydrogenase-deficient granulocytes. FEBS Lett. 436, 411–414.
van der Hoeven, R., Cruz, M.R., Chavez, V., Garsin, D.A., 2015. Localization of the Dual Oxidase BLI-3 and Characterization of Its NADPH Oxidase Domain during Infection of Caenorhabditis elegans. PLoS ONE 10, e0124091.
Vega, N.M., Allison, K.R., Samuels, A.N., Klempner, M.S., Collins, J.J., 2013. Salmonella typhimurium intercepts Escherichia coli signaling to enhance antibiotic tolerance. Proc. Natl. Acad. Sci. U. S. A. 110, 14420–14425.
Vives Corrons, J.L., Feliu, E., Pujades, M.A., Cardellach, F., Rozman, C., Carreras, A., Jou, J.M., Vallespi, M.T., Zuazu, F.J., 1982. Severe-glucose-6-phosphate dehydrogenase (G6PD) deficiency associated with chronic hemolytic anemia, granulocyte dysfunction, and increased susceptibility to infections: description of a new molecular variant (G6PD Barcelona). Blood 59, 428–434.
Yang, H.C., Chen, T.L., Wu, Y.H., Cheng, K.P., Lin, Y.H., Cheng, M.L., Ho, H.Y., Lo, S.J., Chiu, D.T., 2013. Glucose 6-phosphate dehydrogenase deficiency enhances germ cell apoptosis and causes defective embryogenesis in Caenorhabditis elegans. Cell Death. Dis. 4, e616.
Yang, H.C., Ma, T.H., Tjong, W.Y., Stern, A., Chiu, D.T., 2021. G6PD deficiency, redox homeostasis, and viral infections: implications for SARS-CoV-2 (COVID-19). Free Radic. Res. 55, 364–374.
Yang, H.C., Wu, Y.H., Yen, W.C., Liu, H.Y., Hwang, T.L., Stern, A., Chiu, D.T., 2019. The redox role of G6PD in cell growth, cell death, and cancer. Cells 8.
Yang, H.C., Yu, H., Ma, T.H., Tjong, W.Y., Stern, A., Chiu, D.T., 2020. tert-Butyl Hydroperoxide (tBHP)-Induced Lipid Peroxidation and Embryonic Defects Resemble Glucose-6-Phosphate Dehydrogenase (G6PD) Deficiency in C. elegans. Int. J. Mol. Sci. 21.
Yen, W.C., Wu, Y.H., Wu, C.C., Lin, H.R., Stern, A., Chen, S.H., Shu, J.C., Tsun-Yee Chiu, D., 2020. Impaired inflammasome activation and bacterial clearance in G6PD deficiency due to defective NOX/p38 MAPK/AP-1 redox signaling. Redox. Biol. 28, 101363.